Identification of the Sites of Incorporation of [^{3}H]Ethidium Diazide within the Torpedo Nicotinic Acetylcholine Receptor Ion Channel†

Megan B. Pratt,‡ Steen E. Pedersen,§ and Jonathan B. Cohen*,‡

Department of Neurobiology, Harvard Medical School, 220 Longwood Avenue, Boston, Massachusetts 02115, and Department of Molecular Physiology and Biophysics, Baylor College of Medicine, Houston, Texas 77030

Received May 23, 2000; Revised Manuscript Received June 28, 2000

ABSTRACT: The binding sites of ethidium, a noncompetitive antagonist of the nicotinic acetylcholine receptor (nAChR), have been localized in the *Torpedo* nAChR in the desensitized state by use of a photoactivatible derivative, [^{3}H]ethidium diazide. At 10 μM [^{3}H]ethidium diazide, incorporation into the α-, β-, and δ-subunits was inhibited by the presence of phencyclidine (PCP). Within the α-subunit, the incorporation was mapped to a 20-kDa fragment beginning at αSer-173 and containing the first three transmembrane segments, αM1, αM2, and αM3. Further digestion of this fragment generated two fragments with PCP-inhibitable incorporation, one containing αM1 and one containing both αM2 and αM3. Within αM2, specific incorporation was present in αLeu-251 and αSer-252, residues that have been previously shown to line the lumen of the ion channel. Digestion of the δ-subunit with *S. aureus* V8 protease generated a 14-kDa and a 20-kDa fragment, both of which began at Ile-192 and contained PCP-inhibitable labeling. The 14-kDa fragment, containing δM1 and δM2, was further digested to generate a 3-kDa fragment, containing δM2 alone, with PCP-inhibitable incorporation. Digestion of the 20-kDa fragment, which contained δM1, δM2, and δM3, generated two fragments with incorporation, one containing the δM1 segment and the other containing δM2 and δM3. These results establish that in the desensitized state of the nAChR, the high-affinity binding site of ethidium is within the lumen of the ion channel and that the bound drug is in contact with amino acids from both the M1 and M2 hydrophobic segments.

The *Torpedo* nicotinic acetylcholine (nAChR[1]) is composed of four homologous subunits (α, β, γ, δ) arranged pseudosymmetrically around a central ion pore. Each subunit consists of a large extracellular N-terminal segment, four transmembrane segments, M1−M4, and a cytoplasmic segment between M3 and M4. The extracellular domain contains the two agonist binding sites, located at the interfaces of the α−γ and α−δ subunits with residues from each contributing. The M2 segment of each subunit is α-helical and lines the lumen of the channel, with an additional contribution from the M1 segments (*1*−*3*).

The aromatic amines are the most studied structural class of the diverse group of compounds that act as noncompetitive antagonists (NCAs) on the nAChR. Affinity labeling and electrophysiology experiments show that many of these drugs bind in the ion channel. Mutations within M2 affect the potency of QX222 block (*4*), and mutations in M1 affect quinacrine block (*5*). Photoaffinity labeling studies established that, in the desensitized state, [^{3}H]chlorpromazine, [^{3}H]-triphenylmethylphosphonium, and [^{3}H]meproadifen mustard all label residues within M2 (*6*−*8*), while [^{3}H]tetracaine is photoincorporated into M2 residues in the resting state (*9*). In the open channel state, [^{3}H]quinacrine azide labels residues in M1 (*10, 11*). All of the residues that have been labeled by these NCAs are accessible to water-soluble modification agents, consistent with these residues forming a portion of the channel (*12*). Additionally, all of these compounds bind competitively with [^{3}H]phencyclidine (PCP) or [^{3}H]histrionicotoxin (HTX), two other aromatic amine NCAs, consistent with a common site of action.

Although known primarily for its ability to intercalate into DNA, the fluorescent compound ethidium is another aromatic amine NCA of the nAChR, which binds competitively with PCP and HTX. The affinity of ethidium for the nAChR in the desensitized state has been determined, with a K_i of 0.4−0.6 μM based on inhibition of [^{3}H]PCP binding (*13, 14*) or a K_i of 0.3−0.8 μM based on inhibition by PCP of the fluorescence of bound ethidium (*13, 15*). In contrast to the high-affinity binding to the nAChR in the desensitized state, in the presence of α-bungarotoxin (αBgTx), ethidium inhibits [^{3}H]PCP binding with a K_i of 1 mM (*13*). Ethidium also binds the agonist site, with an affinity for the α−γ site of ∼5 μM and for the α−δ site of ∼100 μM (*14*).

† This research was supported in part by United States Public Health Service Grants NS19522 (J.B.C.) and NS35212 (S.E.P.) and by an award in Structural Neurobiology from the Keck Foundation. M.B.P. was supported in part by Training Grant NS07112.

* To whom correspondence should be addressed. Tel: (617)432-1728. Fax: (617)734-7557. E-mail: jonathan_cohen@hms.harvard.edu.

‡ Harvard Medical School.

§ Baylor College of Medicine.

[1] Abbreviations: nAChR, nicotinic acetylcholine receptor; NCA, noncompetitive antagonist; CPZ, chlorpromazine; PCP, phencyclidine; HTX, *dl*-perhydrohistionicotoxin; αBgTx, α-bungarotoxin; dTC, *d*-tubocurarine; FRET, fluorescence resonance energy transfer; PAGE, polyacrylamide gel electrophoresis; EndoLysC, endoproteinase Lys-C; 1-AP, 1-azidopyrene; V8 protease, *S. aureus* glutamyl endopeptidase; TFA, trifluoroacetic acid; PTH, phenylthiohydantoin; TPS, *Torpedo* physiological saline; GSSG, oxidized glutathione.

10.1021/bi0011680 CCC: $19.00
Published on Web 08/22/2000

The fluorescence of ethidium has made it an attractive probe in fluorescence quenching and fluorescence resonance energy transfer studies of the dimensions of the *Torpedo* nAChR. Initial reports, such as the measured distance between the agonist site and the ethidium NCA site, were consistent with the binding site of ethidium in the channel (*16*). However, subsequent work, using the fluorescent membrane probe C_{12}-Texas Red to measure the distance between the membrane surface and the HTX-sensitive ethidium binding site, placed ethidium ~50 Å from the lipid headgroups. This result suggested that the high-affinity ethidium binding site in the *Torpedo* nAChR in the desensitized state is near the most extracellular portion of the nAChR (*17*).

Another experimental approach to localizing the binding site of ethidium, using photoaffinity probes, has also been attempted. Early work by Witzemann and Raftery (*18*) showed that photoincorporation of [^{3}H]ethidium diazide, a photoactivatible derivative of ethidium, into the α- and δ-subunits of the *Torpedo* nAChR in the desensitized state was inhibitable by HTX. Later, Pedersen (*14*) assayed the incorporation of nonradioactive ethidium diazide, as well as two ethidium monoazides, into the nAChR by the fluorescence of subunits in the SDS−PAGE gel. In the absence of agonist, the most prominent incorporation into the nAChR was in the α- and γ-subunits. This incorporation was reduced by ~80% by the presence of carbamylcholine, but the addition of NCAs in the presence of carbamylcholine decreased the photoincorporation little, if at all. However, the ethidium analogues competitively inhibit the binding of [^{3}H]PCP, similarly to ethidium. Based on the work by Witzemann and Raftery (*18*), it is most likely that, once the ethidium azides incorporate into the NCA site, the fluorescence is no longer detectable.

Here we utilized [^{3}H]ethidium diazide to localize the NCA binding site of ethidium. The photoincorporation of [^{3}H]-ethidium diazide into the subunits of the *Torpedo* nAChR reflected the general pharmacology of [^{3}H]ethidium binding. For nAChR equilibrated with carbamylcholine, in the desensitized state, the addition of PCP reduced the incorporation into the α- and δ-subunits. [^{3}H]Ethidium diazide photoincorporated into the M2 segments of the α- and δ-subunits, as well as into fragments containing the M1 segment of the α- and δ-subunits, indicating a binding site in the channel pore. These results lead us to conclude that the high-affinity ethidium binding site in the nAChR in the desensitized state is within the channel domain of the nAChR and not in the extracellular domain.

EXPERIMENTAL PROCEDURES

Materials. nAChR-enriched membranes were isolated from *Torpedo californica* electric organ according to the method described by Pedersen et al. (*8*). The final membrane suspensions were stored in 38% sucrose at −80 °C under argon. The membranes used here contained 0.5−2.0 nmol of [^{3}H]acetylcholine binding sites/mg of protein. [^{3}H]-Ethidium (specific activity: 1.15 Ci/mmol) and [^{3}H]ethidium diazide (specific activity: 0.61 Ci/mmol) were synthesized according to the methods described by Pedersen (*14*) and Lurtz et al. (*15*). Azidopyrene (1-AP) was from Molecular Probes. Oxidized glutathione, carbamylcholine, nonradioactive ethidium, and Tricine were from Sigma. *Staphylococcus aureus* glutamyl endopeptidase (V8 protease) was from ICN Biomedical. Endoproteinase-Lys-C (EndoLysC), which cleaves at the C-terminal side of lysines except before prolines, was from Boehringer Mannheim. Phencyclidine (PCP) was purchased from Alltech Associates. *d*-Tubocurarine (dTC) was from Sigma, and α-bungarotoxin (αBgTx) was from Biotoxins. Endoglycosidase H was from Genzyme.

Equilibrium Binding Assay. nAChR-rich membranes (~900 nM ACh sites) in *Torpedo* physiological saline (250 mM NaCl, 5 mM KCl, 3 mM $CaCl_2$, 2 mM $MgCl_2$, 5 mM sodium phosphate, pH 7.0; TPS) were incubated for 2 h at room temperature with varying concentrations of [^{3}H]ethidium in the presence or absence of other cholinergic drugs. After incubation, the membrane suspensions (90 μL) were filtered through 13-mm glass fiber filters (Schleicher & Schuell #32) which were pretreated with 1% Prosil (Lancaster) to reduce nonspecific binding. The filters were washed with 2 mL of TPS and dried. The free concentration (*F*) was determined by scintillation counting of an aliquot of the filtrate, while the bound concentration (*B*) was determined from the filters. The data were fit to eq 1:

$$B = \frac{B_{max} \times F}{K_{eq} + F} + B_{ns} \times F \quad (1)$$

where B_{max} is the maximum number of binding sites, K_{eq} is the concentration of [^{3}H]ethidium at which one-half of the available sites are bound, and B_{ns} is the nonspecific binding. B_{ns} was determined from a linear fit of the binding in the presence of carbamylcholine and PCP. The fit was calculated from duplicate samples using SigmaPlot.

Photoaffinity Labeling of nAChR-Enriched Membranes with [^{3}H]Ethidium Diazide. For analytical labeling experiments, freshly thawed *Torpedo* membranes were diluted with TPS and pelleted (15000*g*) for 30 min. The pellets were resuspended in TPS (2 mg protein/mL; ~1 μM nAChR), and [^{3}H]ethidium diazide (10 μM) was added. The membrane suspensions were split into aliquots (100 μg/condition), and additional ligands were added to the final concentrations indicated in the figure legends. After a 1-h incubation at room temperature, oxidized glutathione (GSSG) was typically added to a final concentration of 10 mM. The suspensions were irradiated at 254 nm (Spectroline EF-16) for 30 s in a plastic 96-well plate on ice. Photolysis for an additional 90 s did not increase the incorporation appreciably. The suspensions were diluted with sample loading buffer and directly submitted to SDS−PAGE.

For proteolytic mapping of [^{3}H]ethidium diazide-labeled α-subunit with *S. aureus* V8 protease (*19*), labeling was carried out with 800 μg (analytical mapping) or 10 mg (preparative) of nAChR-rich membranes. For analytical mapping, samples were photolyzed in a 24-well plate, whereas for preparative mapping, the samples were photolyzed in two glass crystallization dishes per condition (3-cm i.d.). Following photolysis, the membranes were collected by centrifugation. For analytical mapping, samples were resuspended in 80 μL of 50 mM sodium phosphate, pH 7, 1% SDS. Samples were divided in half, and 40 μL of 50 mM sodium phosphate, pH 6, with or without 5 mU Endoglycosidase H, was added to each. After an overnight incubation, samples were diluted with sample buffer and

submitted to SDS−PAGE. For preparative mapping, samples were resuspended in TPS (2 mg/mL) after photolysis and centrifugation. The samples were then further labeled with 1-AP (*20*) to ease identification and isolation of subunits and fragments from gels. 1-AP (62.5 mM in DMSO) was added to a final concentration of 500 μM. After a 90-min incubation, the samples were photolyzed for 15 min on ice using a 365-nm lamp (Spectroline EN-16). Membranes were pelleted (15000*g*) for 30 min, resuspended in sample buffer, and submitted to SDS−PAGE.

Gel Electrophoresis. SDS−PAGE was performed as described by Pedersen et al. (*19*). For analytical gels, the polypeptides were resolved on a 1-mm thick, 8% acrylamide gel and visualized by staining with Coomassie Blue (0.25% w/v in 45% methanol and 10% acetic acid). For autoradiography, the gels were impregnated with fluor (Amplify, Amersham), dried, and exposed at −80 °C to Kodak X-OMAT film for various times (6−8 weeks). Additionally, incorporation of ^{3}H into individual polypeptides was quantified by scintillation counting of excised gel slices, as described by Middleton and Cohen (*21*). For analytical V8 mapping gels, following electrophoresis, the gel was briefly stained with Coomassie Blue and destained to allow visualization of the subunits. The subunits were then excised and placed directly into individual wells of a 1.5-mm mapping gel, composed of a 5-cm, 4.5% acrylamide stacking gel, and a 15-cm, 15% acrylamide separating gel. Into each well was added 1:1 g of subunit:g of *S. aureus* V8 protease in overlay buffer (5% sucrose, 125 mM Tris-HCl, 0.1% SDS, pH 6.8). The gel was electrophoresed at 150 V for 2 h, and then the current was turned off for 1 h. The gel was then run at constant current overnight until the dye front reached the end of the gel. The gel was stained, and the ^{3}H was quantified by liquid scintillation counting. For preparative labelings, the polypeptides were resolved on a 1.5-mm thick, 8% acrylamide gel. The α- and δ-subunits were identified in the 8% gels by 1-AP fluorescence, excised, and loaded directly onto the 1.5-mm mapping gels. The α-subunit proteolytic fragment of ∼20 kDa (αV8-20) was identified by fluorescence (*20*) and excised. Fluorescent bands near ∼14 kDa (δV8-14) and ∼20 kDa (δV8-20), as well as areas containing no fluorescence, were excised from the V8 mapping gel of δ-subunit. The excised proteolytic fragments were isolated by passive elution into 0.1 M NH_4HCO_4, 0.1% SDS. The eluate was filtered (Whatman No. 1) and concentrated using Millipore 5K concentrators. To remove excess SDS, acetone was added to the concentrate, and following incubation at −20 °C overnight, the peptides were pelleted.

EndoLysC Digest. For EndoLysC digestion, acetone-precipitated peptides isolated from the mapping gels were resuspended in 15 mM Tris, pH 8.1, 0.1% SDS. EndoLysC (1.5 mU in resuspension buffer) was added to a final volume of 100 μL. The digestion was allowed to proceed for 7−9 days before either purification of fragments by HPLC or separation of fragments by Tricine SDS−PAGE (*20*, *22*). ^{3}H in the Tricine gel was quantified by cutting the gel into 2-mm sections throughout the length of the gel. The ^{3}H in each slice was counted as described in the previous section.

HPLC Purification. Proteolytic fragments from enzymatic digestion of [^{3}H]ethidium diazide-labeled subunits were further purified by reverse-phase HPLC, as described by Blanton and Cohen (*20*), using a Brownlee C4 Aquapore column (100 × 2.1 mm; 7-μm particle size). Solvent A was 0.08% TFA in water, and solvent B was 0.05% TFA in 60% acetonitrile/40% 2-propanol. A nonlinear gradient (Waters model 680 gradient controller, curve No. 7) from 25% to 100% solvent B in 80 min was used. The rate of flow was 0.2 mL/min, and 0.5-mL fractions were collected. The elution of peptides was monitored by absorbance at 215 nm, and the fluorescence from 1-AP was detected by fluorescence emission (357 nm excitation, 432 nm emission). Additionally, aliquots from the fractions were taken to determine ^{3}H by liquid scintillation counting.

Amino-Terminal Sequence Analysis. Automated amino-terminal sequence analysis was performed on an Applied Biosystems model 477A protein sequencer with an in-line 120A PTH analyzer. HPLC samples (450 μL) were directly loaded onto chemically modified glass fiber disks (Beckman) in 20-μL aliquots, allowing the solvent to evaporate at 40 °C between loads. Sequencing was performed using gas-phase TFA to minimize possible hydrolysis of label from the polypeptide. After conversion of the released amino acids to PTH amino acids, one portion, approximately one-third, went to the PTH analyzer while the remainder was collected for scintillation counting. The samples were counted for three 5-min intervals, and the results were averaged to generate reported errors. Yield of PTH amino acids, along with background-subtracted levels, was calculated from peak height compared with standards using the program Model 610A Data Analysis Program, version 1.2.1. Initial yield and repetitive yield were calculated using SigmaPlot by a nonlinear least-squares regression to the equation $M = I_0 * R^n$, where M is the observed release, I_0 is the initial yield, R is the repetitive yield, and n is the cycle number. Derivatives known to have poor recovery (Ser, Arg, Cys, and His) were omitted from the fit.

RESULTS

Equilibrium Binding of [^{3}H]Ethidium to nAChR-Rich Membranes. To characterize the reversible interactions of ethidium with the nAChR, equilibrium binding of [^{3}H]-ethidium to *Torpedo* nAChR-rich membranes was measured in the presence of cholinergic agonists, competitive antagonists, and noncompetitive antagonists. To quantify binding in the desensitized state, [^{3}H]ethidium binding was measured in the presence of 2 mM carbamylcholine in the presence and absence of 100 μM PCP (Figure 1). The binding in the desensitized state was characterized by binding to a high-affinity site (K_{eq} ∼0.6 μM) as well as a nonspecific component defined by the binding in the presence of PCP, a line with a slope of ∼0.08. This high-affinity binding was similar to literature values, measured both by the inhibition of [^{3}H]PCP binding [K_{eq} ∼0.4−0.6 μM (*13*, *14*)] as well as by the fluorescence of bound ethidium [K_{eq} ∼0.3−0.8 μM (*13*, *15*)]. In the presence of dTC, [^{3}H]ethidium was bound with a similar high affinity to the same number of sites. There was no evidence of high-affinity [^{3}H]ethidium binding in the presence of αBgTx, as the binding in the presence of αBgTx was approximately linear with a slope of ∼0.09, similar to the slope in the presence of carbamylcholine and PCP. Since high-affinity binding of [^{3}H]ethidium was seen when the agonist site was occupied by either agonist or competitive antagonist, [^{3}H]ethidium must bind to a site distinct from the ACh site. The binding at this site was

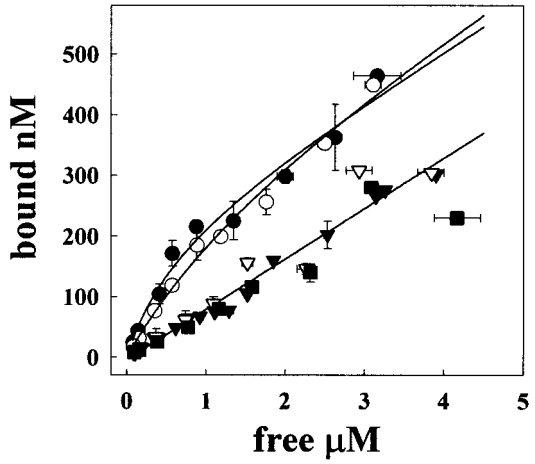

FIGURE 1: Binding of [3H]ethidium in the presence and absence of various cholinergic drugs. nAChR-rich membranes (2 mg/mL with ~900 nM ACh binding sites) were equilibrated with various cholinergic drugs [2 mM carbamylcholine (●), 100 μM dTC (○), 2 mM carbamylcholine with 100 μM PCP (▼), 10 μM αBgTx (▽), or 125 μM ethidium (■)] with increasing concentrations of [3H]-ethidium. After a 2-h incubation, the concentration of bound and free [3H]ethidium was determined by filtration. The points plotted are the averages of duplicate samples. The observed binding in the presence of αBgTx, ethidium, or carbamylcholine with PCP was fit to a line to determine the nonspecific binding (B_{ns}). The specific binding in the presence of carbamylcholine or dTC was determined according to eq 1 in Experimental Procedures. Both B_{max} and K_{eq} were variables, and B_{ns} was determined from the slope of the binding in the presence of carbamylcholine and PCP: +carb, K_{eq} = 0.6 ± 0.3 μM, B_{max} = 200 ± 30 nM; +dTC, K_{eq} = 1.7 ± 0.3 μM, B_{max} = 270 ± 50 nM; +carb/+PCP, slope = 0.083 ± 0.004; +ethidium, slope = 0.065 ± 0.008; +αBgTx, 0.085 ± 0.004.

inhibited by the presence of PCP, indicating that this site was a noncompetitive antagonist site.

Photoincorporation of [3H]Ethidium Diazide into nAChR-Rich Membranes. Initial photoincorporation experiments were designed to determine the general aspects of [3H]-ethidium photoincorporation as well as the effects of agonists and NCAs on the incorporation. nAChR-rich membranes (2 mg/mL) were equilibrated with 10 μM [3H]ethidium diazide in the presence and absence of 2 mM carbamylcholine or 100 μM PCP. These experiments were carried out in the presence of 10 mM GSSG as a scavenger (*9*). Initially, incorporation of 3H was determined by fluorography after SDS−PAGE. In the presence of carbamylcholine, [3H]-ethidium diazide incorporated into all subunits of the nAChR as well as into rapsyn, a 43-kDa protein associated with the cytoplasmic aspect of the nAChR, and the α-subunit of Na^+/K^+ ATPase, a 90-kDa polypeptide from a contaminating membrane fraction (Figure 2). The incorporation in the α-, β-, and δ-subunits was reduced in nAChR equilibrated with PCP.

The effectiveness of GSSG as a scavenger was tested over a range of concentrations. In the presence of carbamylcholine, increasing GSSG concentrations reduced the incorporation in all polypeptides, both in the presence and in the absence of PCP (Figure 3). The incorporation in non-nAChR polypeptides, those running at 37 and 90 kDa [corresponding to calelectrin and the α-subunit of Na^+/K^+ ATPase, respectively (*23*)], was independent of PCP at all concentrations of GSSG. The amount of PCP-inhibitable labeling in the α-, β-, and δ-subunits was approximately constant across the range of GSSG conditions tested. Thus, GSSG reduced the

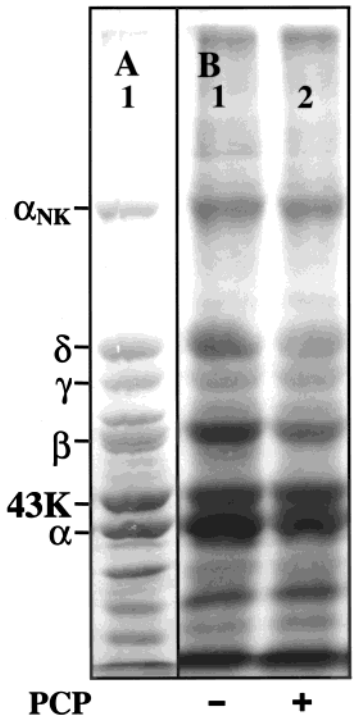

FIGURE 2: Photoincorporation of [3H]ethidium diazide into nAChR-rich membranes. nAChR-rich membranes (100 μg) were equilibrated with [3H]ethidium diazide in TPS (2 mg/mL) in the presence of 10 mM GSSG and 2 mM carbamylcholine and in the absence (lane 1) or presence (lane 2) of 100 μM PCP. After photolysis at 265 nm for 30 s, the samples were subjected to SDS−PAGE, visualized by Coomassie Blue (A), processed for fluorography, and exposed to film for 6 weeks (B). Indicated on the left are the mobilities of the nAChR subunits, rapsyn (43K), and the α-subunit of the Na^+/K^+ ATPase (αNK).

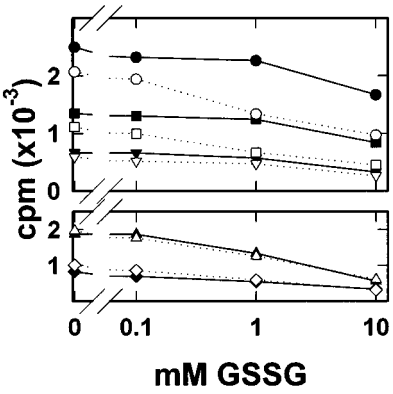

FIGURE 3: Effects of GSSG on [3H]ethidium diazide photoincorporation into nAChR-rich membranes. nAChR-rich membranes (100 μg) were equilibrated with [3H]ethidium diazide in TPS (2 mg/mL) in the presence of 2 mM carbamylcholine without (solid symbols) or with (open symbols) 100 μM PCP and with GSSG from 0 to 10 mM. After photolysis at 265 nm for 30 s, samples were subjected to SDS−PAGE and visualized by Coomassie Blue. The nAChR α (●,○), γ (▼,▽), and δ (■,□) subunits as well as bands of 37 kDa (calelectrin, ◆,◇) and 90 kDa (α-subunit of Na^+/K^+ ATPase, ▲,△) were excised. 3H was quantified by scintillation counting.

nonspecific incorporation into the polypeptides, but not the specific labeling, and therefore, 10 mM GSSG was included in all subsequent experiments.

The effects of carbamylcholine, PCP, and several other drugs were studied by quantification of 3H in bands excised from a gel (Figure 4). In addition to the bands containing

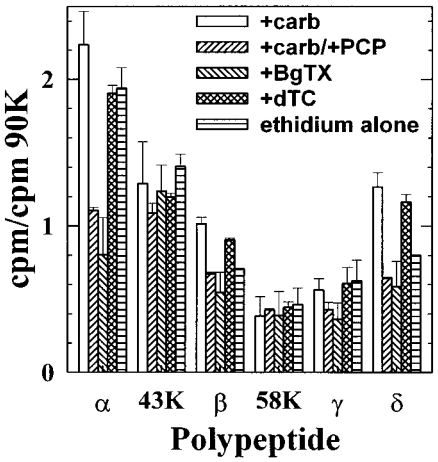

FIGURE 4: Photoincorporation of [^{3}H]ethidium diazide into nAChR-rich membranes in the presence of various cholinergic drugs. nAChR-rich membranes (100 μg) were equilibrated with [^{3}H]-ethidium diazide in TPS (2 mg/mL) in the presence of 10 mM GSSG and in the presence of 2 mM carbamylcholine, 2 mM carbamylcholine and 100 μM PCP, 10 μM αBgTx, 100 μM dTC, or no other drug. After photolysis at 265 nm for 30 s, samples were subjected to SDS−PAGE and visualized by Coomassie Blue. Bands corresponding to indicated polypeptides, as well as a 90-kDa band, containing the α-subunit of Na^+/K^+ ATPase, were excised. ^{3}H was quantified by scintillation counting. Values are the average from duplicate lanes for each condition, with the ^{3}H normalized with respect to that in the 90-kDa band, to reduce variability between lanes. Average ^{3}H incorporation (cpm) in polypeptides labeled in the presence of carbamylcholine (+/−) or in the presence of carbamylcholine and PCP (+/+): α-subunit (+/−) 2098 ± 27, (+/+) 1278 ± 310; δ-subunit (+/−) 1186 ± 15, (+/+) 740 ± 159; β-subunit (+/−) 952 ± 44, (+/+) 775 ± 161. For αNK: (+/−) 942 ± 84, (+/+) 1154 ± 256.

the nAChR subunits, non-nAChR polypeptides were excised as controls. The presence of cholinergic agonists and antagonists did not affect the incorporation into two bands containing non-nAChR polypeptides: a band at 43 kDa, containing the protein rapsyn, and one at 58 kDa, containing syntrophin, a protein of the dystrophin complex (*23*). For membranes equilibrated with carbamylcholine, the incorporation of [^{3}H]ethidium diazide in the α- and δ-subunits was reduced by 40% by PCP, whereas the incorporation was reduced 30% in the β-subunit. Although the incorporation in the γ-subunit was low, the incorporation also appeared reduced by the presence of PCP. As was seen for [^{3}H]-ethidium binding to the nAChR, nAChR subunit labeling by [^{3}H]ethidium diazide in the presence of αBgTx was similar to that in the presence of both carbamylcholine and PCP in all subunits. The incorporation in the presence of dTC was similar to that seen with carbamylcholine, consistent with the comparable binding affinity of [^{3}H]ethidium in the presence of these drugs. In the absence of other ligands, [^{3}H]-ethidium diazide was expected to incorporate into the agonist site, based on the carbamylcholine sensitivity of the incorporation of ethidium diazide as measured by fluorescence (*14*). However, compared with the incorporation of [^{3}H]-ethidium diazide without other ligands, carbamylcholine increased the labeling of the nAChR β- and δ-subunits, while incorporation in the α-subunit was unchanged. This result was likely due to decreased labeling in the agonist site with a concomitant increase in labeling at the noncompetitive antagonist site. Based upon the total picomoles of nAChR loaded in each gel lane and the observed ^{3}H in the subunit

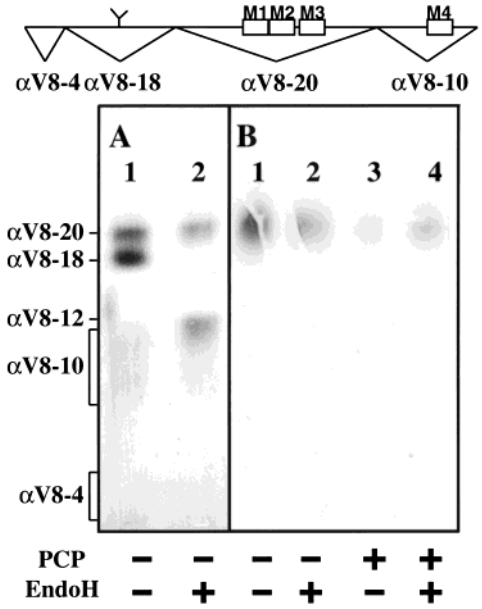

FIGURE 5: Proteolytic mapping of sites of [^{3}H]ethidium diazide incorporation into the nAChR α-subunit using *S. aureus* V8 protease. nAChR-rich membranes (800 μg) were labeled with [^{3}H]-ethidium diazide in the presence of 10 mM GSSG and 2 mM carbamylcholine and in the absence (lanes 1, 2) or presence (lanes 3, 4) of PCP and split for incubation with (lanes 2, 4) or without (lanes 1, 3) Endoglycosidase H as described in Experimental Procedures. After incubation, membranes were submitted to SDS−PAGE, and the α-subunit was excised. The excised bands were transferred to the well of a 15% mapping gel and digested with V8 protease as described: (A) mapping gel stained with Coomassie Blue; (B) fluorogram of mapping gel, exposed for 6 weeks. The mobility of the proteolytic fragments is indicated on the left. Shown above is a schematic indicating the positions of the four fragments within the primary structure of the nAChR α-subunit. ^{3}H incorporation (cpm) in the presence of carbamylcholine (+/−) or in the presence of carbamylcholine and PCP (+/+) in each subunit fragment: αV8-20 (+/−) 2271, (+/+) 832; αV8-18 (+/−) 390, (+/+) 184; αV8-10 (+/−) 346, (+/+) 251; αV8-4 (+/−) 43, (+/+) 26. After treatment with EndoH: αV8-20 (+/−) 1618, (+/+) 533; αV8-18 (+/−) 126, (+/+) 60; αV8-10 (+/−) 320, (+/+) 255; αV8-4 (+/−) 27, (+/+) 20.

gel slice, the total ^{3}H incorporation in α- and δ-subunits in the presence of carbamylcholine was approximately 0.04 mol of [^{3}H]ethidium diazide/mol of subunit, while the incorporation in the presence of both carbamylcholine and PCP was approximately 0.02 mol of [^{3}H]ethidium diazide/mol of subunit. The pattern of labeling indicates that when [^{3}H]-ethidium diazide is bound to its NCA site in the desensitized state of nAChR, it can be photoincorporated into at least the α-, β-, and δ-subunits.

Mapping the [^{3}H]Ethidium Diazide Incorporation in nAChR α-Subunit with S. aureus V8 Protease. To characterize further the site of incorporation, the α-subunit isolated from nAChR labeled in the desensitized state with [^{3}H]-ethidium diazide was subjected to proteolysis with *S. aureus* V8 protease in a mapping gel (Figure 5). V8 protease cleavage in the gel generates four large fragments: αV8-20, αV8-18, αV8-10, and αV8-4, named according to their apparent molecular weights (*19*). αV8-20 (Ser-173−Glu-338) includes the αM1, αM2, and αM3 transmembrane segments, as well as a portion of the N-terminal extracellular segment. The αM4 transmembrane segment is within αV8-10 (Asn-339−αGly-437). αV8-18 (Val-46−Glu-172) contains N-linked glycosylation that is sensitive to cleavage by En-

doglycosidase H; when membranes are treated with Endoglycosidase H, the deglycosylated fragment shifts mobility to ~12 kDa (αV8-12). The autoradiogram shows that the major site of incorporation was in the αV8-20 fragment and that incorporation was inhibited by PCP. Based on counting excised gel fragments, ~75% of the ^{3}H incorporated into the α-subunit labeled in the absence of PCP was in αV8-20, and that incorporation was reduced by ~60% in fragments from nAChR equilibrated with PCP.

Localization of [^{3}H]Ethidium Diazide Incorporation into the α-Subunit. To further characterize the incorporation in the α-subunit, the αV8-20 fragment was further proteolyzed with EndoLysC and subjected to N-terminal amino acid sequencing. 10 mg of nAChR membranes was labeled in the presence of 10 mM GSSG and 2 mM carbamylcholine and in the absence (denoted as +/−) or presence (+/+) of PCP. These membranes were also labeled with 1-AP (*20*) for ease of identifying subunits and fragments following SDS−PAGE, as described in Experimental Procedures. Following separation of subunits by SDS−PAGE, the α-subunit was transferred to the well of a mapping gel for digestion with V8 protease. Proteolytic fragments were identified after electrophoresis by illumination at 365 nm to detect 1-AP incorporation. αV8-20 was identified by fluorescence and mobility, excised, eluted, and concentrated.

To localize the incorporation of [^{3}H]ethidium diazide in αV8-20, αV8-20 was further digested with EndoLysC, which is known to generate a ~10-kDa fragment which begins at αMet-243, the N-terminus of the αM2 segment, and is presumed to continue through αM3 (*8*). There are only three other lysines in αV8-20: two lysines near the beginning of αV8-20 (αLys-185 and αLys-179) and one prior to αM3 (αLys-276). No cleavage has been observed at αLys-276 (*8*, *9*), and Figure 6A shows the expected cleavage products. When the digest was fractionated by HPLC, two hydrophobic peaks, one centered at fraction 29 (~69% organic) and one at fraction 34 (~93% organic), were present (Figure 6B). Additional ^{3}H was not retained on the column, accounting for ~20% of the total ^{3}H eluted from the column. Because similar levels of ^{3}H were present in the flow-through when undigested αV8-20 was chromatographed (Figure 6B, inset), we concluded that this ^{3}H was not associated with a hydrophilic digestion fragment but likely resulted from covalent adducts which were unstable to HPLC conditions or ^{3}H noncovalently associated with αV8-20.

Sequence analyses of fractions 34 of the αV8-20 EndoLysC digests, labeled in the absence and presence of PCP, showed a single sequence beginning at αMet-243 (+/−: I_0 = 109 pmol; +/+: I_0 = 159 pmol) (Figure 7A). No other sequences were detected with more than 5% of the mass of that sequence. For the fragment labeled with [^{3}H]ethidium diazide in the absence of PCP, ~40 cpm were incorporated/pmol of fragment, based on the loaded ^{3}H and the mass present. This incorporation was reduced by ~50% for samples labeled in the presence of PCP. While only low levels of ^{3}H release were seen, the fragment labeled in the absence of PCP showed ^{3}H release reproducibly in cycles 9 and 10, corresponding to αLeu-251 and αSer-252. Additionally, release in cycle 15 was seen, though not reproducibly (compare upper and lower panels of Figure 7A). [^{3}H]-Ethidium diazide incorporated into αLeu-251 at 0.5 cpm/pmol (~0.0009 mol of [^{3}H]ethidium diazide/mol of αLeu-251). ^{3}H was also released in the first cycles, accounting for ~2% of the loaded ^{3}H; this release was likely due to either the loss of poorly absorbed peptide or the instability of the covalent adduct during sequencing conditions. Such loss has also been observed for other photolabel adducts (*24*).

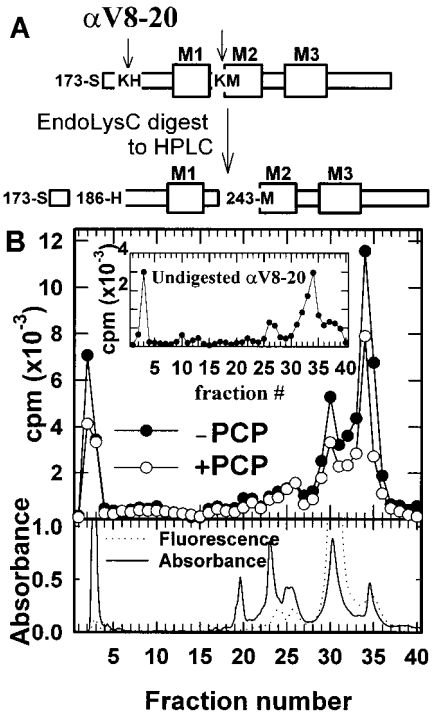

FIGURE 6: Reverse-phase HPLC purification of [^{3}H]ethidium diazide-labeled fragments from EndoLysC digest of αV8-20. (A) Schematic representation of the amino acid sequence of the nAChR α-subunit contained within αV8-20: rectangles, M1, M2, and M3 hydrophobic segments; arrows, location of two known sites of EndoLysC cleavage. The resulting cleavage products are indicated. (B) EndoLysC-digested αV8-20 isolated from nAChR-rich membranes photolabeled with [^{3}H]ethidium diazide in the presence of carbamylcholine and the absence (●) or presence of PCP (○). The digest was applied to a Brownlee Aquapore C4 column and fractionated by reverse-phase HPLC: upper panel, ^{3}H elution profiles (total counts, based on counting 10% of each fraction); lower panel, fluorescence (···) and absorbance profiles (—); inset, ^{3}H elution profile when αV8-20 (+/−) isolated by SDS−PAGE was purified by reverse-phase HPLC.

Sequence analysis of fraction 29 (Figure 7B) revealed the presence of two α-subunit fragments: one beginning at αHis-186 and a secondary sequence beginning at αAsp-180. Both of these fragments must have contained the αM1 segment since there is no other lysine between αHis-186 and αLys-242, prior to αM2. No additional sequences with more than 5% of the mass of the primary sequence were observed. Based on the ^{3}H loaded and the mass levels of the two fragments, ~40 cpm/pmol was incorporated into the fragments in the absence of PCP. This incorporation was reduced by ~60% in fragments labeled in the presence of PCP. The sequence analyses of these fractions from both labeling conditions showed no release of ^{3}H after 25 cycles of Edman degradation, except for the progressively declining release in the first three cycles. The region sequenced contained part of the ACh site (α190−200) but ends prior to M1. The lack of release could be due to either instability of the covalent adduct or labeling at a residue further than 25 amino acids from the N-terminus. For example, if the incorporation were

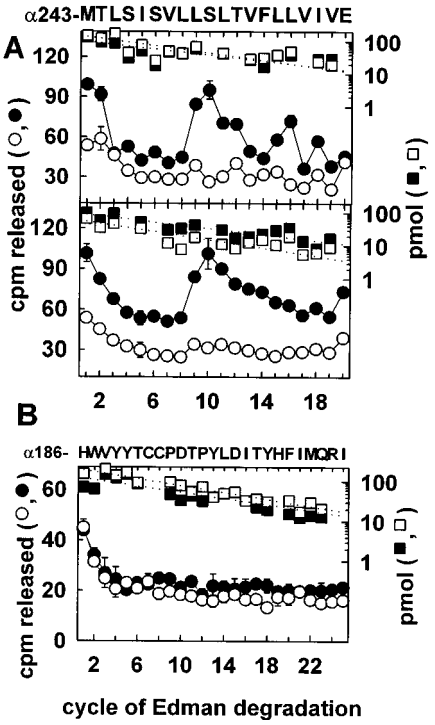

FIGURE 7: ^{3}H and mass release upon N-terminal sequence analysis of HPLC fractions of EndoLysC digest of [^{3}H]ethidium diazide-labeled αV8-20. (A) Sequence analysis of fraction 34 from HPLC purification of EndoLysC digest of [^{3}H]ethidium diazide-labeled αV8-20 from two separate labeling experiments. For each sample, 67% of each cycle of Edman degradation was analyzed for released ^{3}H (●,○) and 33% for released PTH-amino acids (■,□). For both labeling experiments, the only sequence detected began at αMet-243, the N-terminus of αM2. Upper panel (HPLC shown in Figure 6): +/− (●,■) I_0 = 109 pmol, R = 90%, 11600 cpm loaded, 2600 cpm remaining after 25 cycles; +/+ (○,□) I_0 = 159 pmol, R = 88%, 7900 cpm loaded, 1800 cpm remaining after 25 cycles. Lower panel (HPLC not shown): +/− (●,■) I_0 = 98 pmol, R = 90%, 17000 cpm loaded, 5300 cpm remaining after 25 cycles; +/+ (○,□) I_0 = 63 pmol, R = 87%, 7000 cpm loaded, 2500 cpm remaining after 25 cycles. The sequence of the identified peptide is shown above. (B) Sequence analysis of fraction 29 from HPLC purification of Figure 6. As above, for each sample, 67% of each cycle of Edman degradation was analyzed for released ^{3}H (●,○) and 33% for released PTH-amino acids (■,□). For both labeling conditions, the primary sequence detected began at αHis-186 and a secondary sequence beginning at αAsp-180: +/− (●,■) αHis-186 I_0 = 128 pmol, R = 92%, αAsp-180 I_0 = 18 pmol, R = 94%, 5290 cpm loaded, 1250 cpm remaining after 25 cycles; +/+ (○,□) αHis-186 I_0 = 208 pmol, R = 91%, αAsp-180 I_0 = 39 pmol, R = 91%, 3330 cpm loaded, 770 cpm remaining after 25 cycles. Level of released PTH-amino acids of the primary sequence is plotted (■,□), and the sequence of the primary peptide is shown above.

in the αM1 segment, which begins at α211, 25 residues from the N-terminus of this fragment, no release would have been seen.

Localization of [^{3}H]Ethidium Diazide Incorporation into the δ-Subunit. In-gel digestion of nAChR δ-subunit with V8 protease is known to create two fragments with N-termini of δIle-192. One fragment, of approximately 20 kDa (δV8-20), contains the δM1, δM2, and δM3 segments (*20*). The second fragment, of ∼14 kDa (δV8-14), ends at δGlu-262 (*25*) and, therefore, contains the δM1 and δM2 segments but not δM3. When the sites of [^{3}H]ethidium diazide incorporation in the δ-subunit were mapped on an analytical scale by in gel digestion with V8 protease, PCP-inhibitable labeling was seen in bands centered at ∼20 and ∼12 kDa

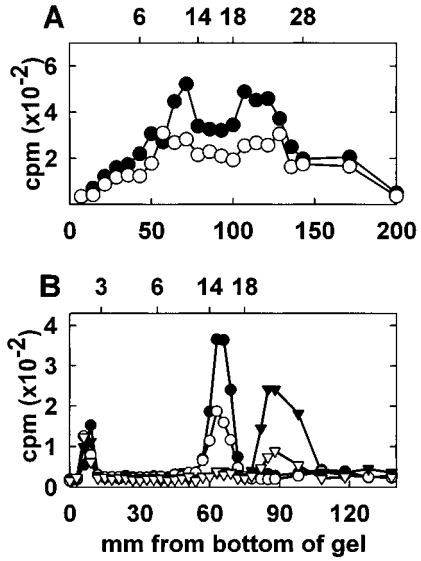

FIGURE 8: Proteolytic mapping of the sites of [^{3}H]ethidium diazide incorporation in the nAChR δ-subunit using V8 protease. (A) nAChR-rich membranes (400 μg) were equilibrated with [^{3}H]-ethidium diazide in TPS in the presence of carbamylcholine and the absence (●) or presence (○) of PCP. After photolysis in the presence of 10 mM GSSG, the samples were subjected to SDS−PAGE and the δ-subunit was excised after brief staining with Coomassie Blue. The excised bands were transferred to the wells of a 15% mapping gel and digested with V8 protease. The lanes were cut into 5-mm slices for the lower and 100 mm and into 20-mm slices for the upper portion of the gel. ^{3}H was quantified by scintillation counting. The mobilities of molecular weight markers are indicated along the top axis. (B) Aliquots of the ∼14 kDa (δV8-14, ●,○) and the ∼20 kDa (δV8-20, ▼,▽) bands eluted from V8 mapping gel of nAChR δ-subunit labeled in the absence (●,▼) and presence (○,▽) of PCP were diluted in sample buffer and submitted to SDS−PAGE using a 15% mapping gel without V8 protease. Gel was run at constant current overnight until dye front reached the bottom of the gel. Lanes were cut into 2-mm slices, and ^{3}H was quantified by scintillation counting. The mobilities of molecular weight markers are indicated along the top axis.

(Figure 8A).

To identify the sites of incorporation of [^{3}H]ethidium diazide in the nAChR δ-subunit, 10 mg of nAChR-rich membrane was photolabeled with [^{3}H]ethidium diazide in the absence or presence of PCP followed by labeling with 1-AP. The subunits were separated by SDS−PAGE, and the δ-subunit was excised and digested with *S. aureus* V8 protease in a mapping gel. After digestion of δ-subunit by V8 protease in the mapping gel, the mobility of digestion products was identified by 1-AP fluorescence. Two fluorescent bands, with estimated mobility near 14 kDa (δV8-14) and 20 kDa (δV8-20) were excised, eluted, and resuspended, as were other fluorescent bands and nonfluorescent regions of the gel. The two noted fluorescent bands contained ∼20% and ∼30% of the total eluted ^{3}H, respectively, as well as the greatest PCP-inhibitable incorporation. Aliquots from these two bands were run on a mapping gel without V8 protease to clearly determine the molecular weight (Figure 8B). While all lanes contained similar ^{3}H in the dye front, the specifically labeled material from the δV8-14 band ran near 14 kDa and that from the δV8-20 band ran near 20 kDa. The material in these two bands was used in subsequent digestions.

Digestion of nAChR δ-subunit with EndoLysC results in cleavage before δMet-257, the N-terminus of δM2, with no

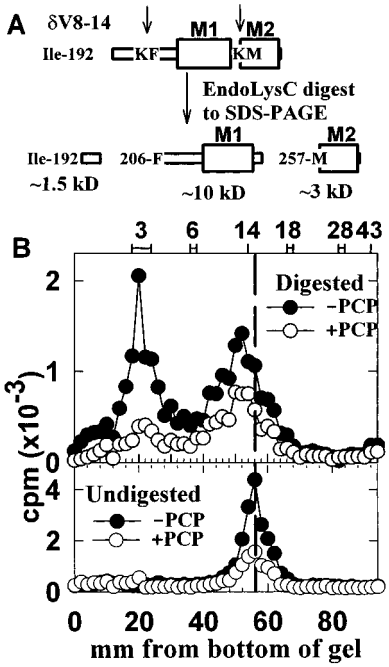

FIGURE 9: Tricine SDS−PAGE fractionation of EndoLysC digest of [3H]ethidium diazide-labeled δV8-14. (A) Schematic representation of δV8-14 sequence: rectangles, δM1 and δM2 segments; arrows, location of two potential sites of EndoLysC cleavage. The resulting cleavage products are indicated. (B) Aliquots of δV8-14 labeled in the absence (●) and presence (○) of PCP were fractionated by Tricine SDS−PAGE. The lanes were cut into 2-mm slices, and 3H incorporation was quantified by scintillation counting: upper panel, EndoLysC digest of δV8-14; lower panel, undigested δV8-14. Mobilities of molecular weight markers are indicated along top axis.

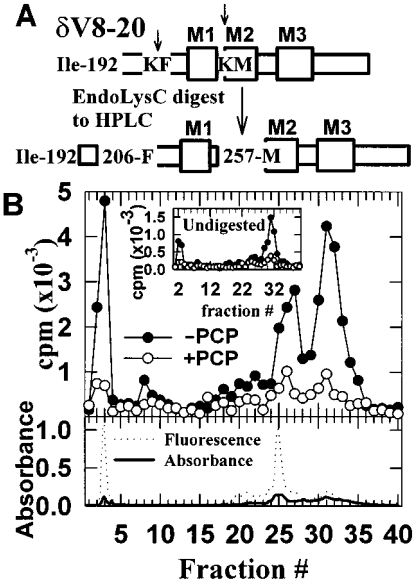

FIGURE 10: Reverse-phase HPLC purification of [3H]ethidium diazide-labeled fragments from EndoLysC digest of δV8-20. (A) Schematic representation of δV8-20: rectangles, δM1, δM2, and δM3 segments; arrows, location of two potential sites of EndoLysC cleavage. The resulting cleavage products are indicated. (B) EndoLysC digests of δV8-20 labeled with [3H]ethidium diazide in the presence of carbamylcholine and the absence (●) and presence (○) of PCP were fractionated by reverse-phase HPLC: upper panel, 3H elution profiles (10% of each fraction counted); inset, 3H elution profile of undigested δV8-20 labeled in the absence (●) and presence (○) of PCP; lower panel, fluorescence (···) and absorbance profiles (—).

cleavage observed after δLys-290, at the N-terminus of M3 (*9*). We used EndoLysC digestion of δV8-14 and δV8-20 to map the sites of [3H]ethidium diazide incorporation into the δ-subunit. Within δV8-14 there are two sites of possible EndoLysC cleavage: δLys-205 and δLys-256. An additional lysine, at δLys-224, precedes a proline, so no cleavage is expected at this site. Therefore, three fragments can be generated by EndoLysC digestion of δV8-14 (Figure 9A): one beginning at δIle-192, with a mobility of ~1.5 kDa; one beginning at δPhe-206, containing a glycosylation site (δAsn-208) (*26*), with a mobility of ~10 kDa; and one beginning at δMet-257 and continuing through δGlu-280, with a mobility of ~3 kDa. Sequence analysis of aliquots of the digest of δV8-14 labeled with [3H]ethidium diazide revealed the presence of two fragments: one beginning at δMet-257 (+/−: I_0 = 3 pmol; +/+: I_0 = 14 pmol) and one beginning at δPhe-206 (+/−: I_0 = 15 pmol; +/+: I_0 = 9 pmol). The fragment beginning at δIle-192 was expected but was not observed; possibly it was lost during sequencing due to its small size. The total digest, as well as undigested δV8-14, was separated by a Tricine SDS−PAGE gel. As shown in Figure 9B, for the digest of δV8-14 labeled in the absence of PCP, the primary peak of 3H was present in a band at ~3 kDa, and this band contained PCP-inhibitable incorporation. The presence of PCP-inhibitable incorporation in the ~3-kDa band indicated that [3H]ethidium diazide photoincorporated into the δM2 segment in a PCP-dependent manner. In addition, the broad band of 3H between 10 and 14 kDa, also containing PCP-inhibitable incorporation, was shifted relative to undigested δV8-14 (lower panel) consistent with the presence of the ~10-kDa fragment beginning at δPhe-206 and ending prior to δM2, as well as possible partially digested products.

Digestion of δV8-20 with EndoLysC is expected to generate three fragments, with N-termini similar to those generated by digestion of δV8-14 with EndoLysC. Cleavage of the lysine at position δLys-290, between the δM2 and δM3 segments, has not been reported. Therefore, the EndoLysC cleavage product beginning at δMet-257 should contain both the δM2 and δM3 segments (Figure 10A). The δV8-20 fragment labeled with [3H]ethidium diazide was digested with EndoLysC and fractionated by HPLC (Figure 10B). PCP-inhibitable incorporation was present in hydrophobic fractions centered at fraction 27 (62% organic) and fraction 31 (78% organic) as well as in the flow-through. Since 3H was also present in the flow-through when intact δV8-20 was repurified by HPLC (Figure 10, inset), as seen with αV8-20, that 3H probably corresponded to label that was unstable to the acidic HPLC conditions, accounting for ~20% of the eluted 3H.

Sequencing of fraction 31 from the HPLC of the samples labeled both in the absence and in the presence of PCP revealed the presence of two sequences: one beginning at δMet-257 (+/−: I_0 = 19 pmol; +/+: I_0 = 6 pmol) and one beginning at δPhe-206 (+/−: I_0 = 27 pmol; +/+: I_0 = 15 pmol) (Figure 11). No 3H release was detected in 25 cycles of Edman degradation, other than the release in the first cycles, accounting for ~3% of the loaded 3H.

Sequence analysis of fraction 27 of the HPLC of EndoLysC-digested δV8-20 labeled with [3H]ethidium diazide in the absence of PCP showed a primary sequence beginning

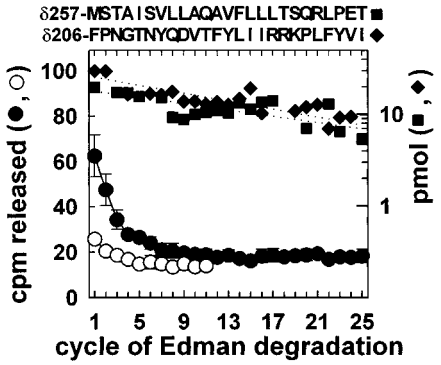

FIGURE 11: Sequence analysis of fragments of δV8-20 produced by EndoLysC digestion. Sequence analysis of fraction 31 from HPLC purification of Figure 10. For each sample, 67% of each cycle of Edman degradation was analyzed for released ^{3}H (●,○) and 33% for released PTH-amino acids (■,◆). For both labeling conditions, two sequences were detected, one beginning at δMet-257, the N-terminus of the M2 segment, and one beginning at δPhe-206. +/− (●): δMet-257, (■) I_0 = 19 pmol, R = 96%; δPhe-206 (◆) I_0 = 27 pmol, R = 95%, 3800 cpm loaded, 1100 cpm remaining after 25 cycles. +/+ (○): δMet-257 I_0 = 5 pmol, R = 99%; δPhe-206 I_0 = 12 pmol, R = 92%, 860 cpm loaded, 170 cpm remaining after 11 cycles. The sequences of the identified peptides are shown above.

at δPhe-206 (I_0 = 53 pmol) with a minor sequence beginning at δMet-257 (I_0 = 4 pmol), present at less than 10% the mass level of the sequence beginning at δPhe-206. As with fraction 31, no release of ^{3}H above background was seen during 25 cycles of sequence analysis (data not shown). Since undigested δV8-20 eluted in fraction 31, the sequence beginning at δPhe-206 in fraction 31 of the HPLC of EndoLysC-digested δV8-20 should contain the M1, M2, and M3 segments. The sequence beginning at δPhe-206 in fraction 27, however, must have been cleaved at the Lys-256, prior to M2. While the ^{3}H release profile provided no information about the site of [^{3}H]ethidium diazide incorporation in the labeled fragments, the presence of PCP-inhibitable incorporation in this HPLC peak indicated that specific incorporation was present within the fragment beginning at δPhe-206, containing M1 without M2.

DISCUSSION

The data presented here localized the specific photoincorporation of [^{3}H]ethidium diazide in the nAChR α- and δ-subunits to both the M2 segment and a fragment containing M1. Previous studies of the incorporation of aromatic amine NCAs into the *Torpedo* nAChR in the desensitized state have shown incorporation into only the M2 segment (*6*−*8*). Additionally, the results reported here have established that, within the α-subunit, αLeu-252 (αLeu-9′) and αSer-253 (αSer-10′), specifically, were labeled by [^{3}H]ethidium diazide. These residues line the lumen of the ion channel (*27*), demonstrating that the high-affinity binding site of ethidium is within the nAChR ion channel.

The pharmacology of the photoincorporation of [^{3}H]-ethidium diazide well-reflected the binding of [^{3}H]ethidium and was similar to that reported by Witzemann and Raftery (*18*). Their data also indicated that, in the desensitized state, the photoincorporation in the α- and δ-subunits was inhibited by the presence of histrionicotoxin, an aromatic amine noncompetitive antagonist. The dependence of subunit photoincorporation on cholinergic ligands reported here, however, was in apparent contrast to that reported by use of fluorescence to detect levels of incorporation of ethidium diazide in subunits after SDS−PAGE (*14*). In that report, the incorporation of ethidium diazide in α- and γ-subunits was reduced by ∼80% by the presence of carbamylcholine, while the addition of PCP produced little or no further change. This contrasts with the present result that carbamylcholine caused no change in ^{3}H incorporation in the α- and γ-subunits, while the presence of PCP inhibited the incorporation in the α-subunit by ∼40%. A likely explanation for the discrepancy is that, surprisingly, in subunits resolved by SDS−PAGE the covalent adduct formed within the ACh binding site remains fluorescent, while the adduct formed in the channel in the α- and δ-subunits is nonfluorescent.

To localize the incorporation in the nAChR to specific fragments of the protein, the α- and δ-subunits were digested first with V8 protease to generate a fragment containing the first three transmembrane segments, and that fragment was then isolated and digested with EndoLysC. In both subunits, two fragments were generated that contained PCP-inhibitable incorporation: one spanning a portion of the extracellular domain through the M1 segment and the other containing the M2 and M3 domains. In the α-subunit, sequence analysis of the fragment containing M2 and M3 established PCP-inhibitable incorporation of [^{3}H]ethidium diazide in αLeu-252 and αSer-253. Thus, in the desensitized nAChR, the high-affinity binding site of ethidium is contained at least in part within the M2 ion channel domain.

Since the site of [^{3}H]ethidium diazide incorporation in the δ-fragment containing δM2 and δM3 was not evident by sequence analysis, the presence of incorporation into the δM2 fragment was determined by alternative means. The δV8-14 fragment, spanning from δIle-192 to δGlu-280, contained a portion of the extracellular segment as well as the δM1 and δM2 segments, but not the δM3 segment. Digestion of this fragment by EndoLysC was expected to generate a 3-kDa fragment consisting solely of the δM2 segment. Separation of the digestion products on an SDS−PAGE gel resulted in a 3-kDa band with associated ^{3}H. Therefore, the M2 segment of δ-subunit was labeled with [^{3}H]ethidium diazide in a PCP-dependent manner. Unfortunately, the specific residues in δM2 labeled with [^{3}H]ethidium diazide could not be determined by sequence analysis. Although many other NCAs which have incorporated into the M2 segments label homologous positions in several subunits (*6*, *7*, *9*, *28*−*30*), sequence analysis failed to provide any evidence of reaction of [^{3}H]ethidium diazide with either δLeu-266 or δSer-267, the homologues to the positions labeled by [^{3}H]ethidium diazide in the α-subunit. However, due to the low mass levels of the δ-subunit fragment observed during sequencing (19 pmol in fraction 31) (Figure 11), incorporation at δLeu-266 at similar levels to αLeu-252 would only have resulted in 6 cpm of release, well below the detection limits of this method.

αLeu-252 and αSer-253 are not necessarily the primary or only sites of labeling in αM2. Approximately 20% of the ^{3}H incorporated into αV8-20 did not remain stably incorporated under the acidic HPLC conditions. Additionally, some of the ^{3}H incorporation was labile to the acid treatment during sequence analysis, as seen by the ^{3}H release detected in the first cycles of sequence analysis. Acid sensitivity was

clearly demonstrated when samples were pretreated with trifluoroacetic acid for 4 min, followed by a wash with ethyl acetate for 5 min to remove excess SDS from the filter prior to sequence analysis. During this treatment, between 10% and 50% of the ^{3}H loaded with a fragment labeled with [^{3}H]-ethidium diazide was released (this prewash was not used in any of the sequences reported here). While as much as 0.04 mol of [^{3}H]ethidium diazide was incorporated/mol of sequence beginning at αMet-243, based on loaded ^{3}H and the mass present, αLeu-252 was only labeled at ~0.0008 mol of [^{3}H]ethidium diazide/mol of residue. Therefore the discrepancy between the ^{3}H incorporated in the fragment and that detected in αLeu-252 was due to either greater incorporation originally at αLeu-252 and αSer-253 or at another site, but this incorporation was labile to the conditions of sequence analysis. Lability of incorporation could also partially account for the lack of release seen in δM2 even though clear evidence of incorporation of [^{3}H]ethidium diazide within the δM2 segment was shown.

This difficulty in localization of the incorporation in the subunits resulted from the sensitivity of the incorporation to the HPLC and sequencing conditions. This sensitivity could be due to the formation of acid-labile adducts upon photolysis. The photoactivatible group used in these experiments, the aryl azide, can undergo an intermolecular rearrangement after photolysis to a ketenimine azepine (*31*). The adducts formed with the azepine are predicted to be sensitive to acid and may account for the loss of ^{3}H during HPLC and sequencing. Another problem with the rearrangement product of the aryl azide is that it is more stable than the initial nitrene. This compound is expected to react preferentially with nucleophiles, such as cysteine. This selective reactivity may pose a problem when the binding site contains no cysteines, as was the case for the M2 segments. However, [^{3}H]ethidium diazide successfully photoincorporated into the M2 segments of α and δ and, particularly, into αLeu-252 and αSer-253.

The binding of ethidium within the M2 channel domain is inconsistent with the site of ethidium binding predicted for the *Torpedo* nAChR from the results of fluorescence resonance energy transfer (FRET). The results of FRET have been interpreted to indicate that, within the desensitized state, the high-affinity ethidium binding site is ~50 Å from the lipid headgroups, within the extracellular domain, well above the transmembrane domain of the nAChR (*17*). However, a binding site within the lumen of the channel could be, within error, ~50 Å from the lipid headgroups. On the basis of the dimensions of the receptor as determined at 9 Å (*32*), the narrowest part of the receptor, near the center of the lipid bilayer, is ~56 Å. This value was used in determining that the ethidium binding site must be outside the lumen of the channel. However, near the lipid headgroups the receptor is wider, ~80 Å (*32*). Therefore, if the distance from the central axis to the outer edge of the receptor is 40 Å and ethidium is binding in the ion channel at the depth equivalent to the middle of the lipid bilayer (~15 Å between the polar headgroups of the phospholipids), then the distance from the ethidium binding site to the lipid headgroups is ~43 Å, close to the calculated distance of ~50 Å.

Although originally proposed to bind far from the other aromatic amine NCAs, [^{3}H]ethidium diazide incorporated into both the M1 and M2 segments, near the other aromatic amine NCAs. Within αM2, [^{3}H]ethidium diazide incorporated into αM2-9′ and αM2-10′ (based on numbering from a conserved lysine at the N-terminus of M2). In the desensitized state, other aromatic amine NCAs, such as [^{3}H]-chlorpromazine and [^{3}H]triphenylmethylphosphonium, labeled residues at the 6′ ring (*7*, *29*), while [^{3}H]meproadifen mustard incorporated into the 20′ ring (*8*). [^{3}H]Quinacrine azide, on the other hand, labeled the M1 segment in the open state (*10*). The structural relation between the M1 and M2 segments is not currently known, but the proximity of these segments to the ethidium binding site indicates that both contribute to the channel pore.

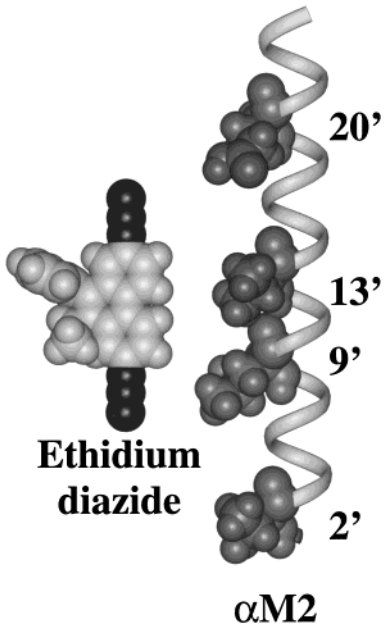

FIGURE 12: Model of ethidium and αM2 helix. α-Helical model of the αM2 segment and space-filling model of ethidium were made using the molecular modeling software Insight (Biosym, Inc.). M2 residues 2′ (threonine), 9′ (leucine), and 20′ (glutamate) are shown as space-filling models, and one azide group of ethidium is positioned in proximity to the αM2 9′ position, which was labeled with [^{3}H]ethidium diazide.

Can the sites of incorporation in the αM2 segment tell us anything about the possible sites of incorporation into the M1 segment? The photoreactive probe used in this study, [^{3}H]ethidium diazide, has two reactive groups, ~9 Å apart (Figure 12). If [^{3}H]ethidium diazide labeled M1 and M2 from a single binding site, then the site of labeling in M1 should be ~9 Å from the sites in M2, αLeu-252, and αSer-253. αLeu-252 and αSer-253 are predicted to be near the center of the bilayer, facing the channel pore. The diameter of an α-helix is 5 Å, and the distance between two residues on the same face of a helix is ~5 Å. Therefore, it is unlikely that [^{3}H]ethidium diazide photoincorporated into the residues implicated in the binding of quinacrine, residues at the most extracellular region of the M1 segment. However, if the M1 segment is α-helical, it is possible that the site of incorporation is approximately midway down the length of the segment, possibly at αVal-218, which has been shown to contribute to channel formation by modification of this position by a water-soluble probe (*12*). Knowledge of the sites of incorporation of [^{3}H]ethidium diazide into the M1 segments will clarify the contribution of the M1 segments to the nAChR ion channel.

REFERENCES

1. Karlin, A., and Akabas, M. H. (1995) *Neuron 15*, 1231−1244.
2. Hucho, F., Tsetlin, V. I., and Machold, J. (1996) *Eur. J. Biochem. 239*, 539−557.
3. Corringer, P.-J., Le Novere, N., and Changeux, J.-P. (2000) *Annu. Rev. Pharmacol. Toxicol. 40*, 431−451.
4. Charnet, P., Labarca, C., Leonard, R. J., Vogelaar, N. J., Czyzyk, L., Gavin, A., Davidsen, N., and Lester, H. A. (1990) *Neuron 2*, 87−95.
5. Tamamizu, S., Todd, A. P., and McNamee, M. G. (1995) *Cell. Mol. Neurobiol. 15*, 427−438.
6. Revah, F., Galzi, J. L., Giraudat, J., Haumont, P.-Y., Lederer, F., and Changeux, J.-P. (1990) *Proc. Natl. Acad. Sci. U.S.A. 87*, 4675−4679.
7. Hucho, F., Oberthur, W., and Lottspeich, F. (1986) *FEBS Lett. 205*, 137−142.
8. Pedersen, S. E., Sharp, S. D., Liu, W.-S., and Cohen, J. B. (1992) *J. Biol. Chem. 267*, 10489−10499.
9. Gallagher, M. J., and Cohen, J. B. (1999) *Mol. Pharmacol. 56*, 300−307.
10. DiPaola, M., Kao, P. N., and Karlin, A. (1990) *J. Biol. Chem. 265*, 11017−11029.
11. Karlin, A. (1991) *The Harvey Lectures 85*, 71−107.
12. Akabas, M. H., and Karlin, A. (1995) *Biochemistry 34*, 12496−12500.
13. Herz, J. M., Johnson, D. A., and Taylor, P. (1987) *J. Biol. Chem. 262*, 7238−7247.
14. Pedersen, S. E. (1995) *Mol. Pharmacol. 47*, 1−9.
15. Lurtz, M. M., Hareland, M. L., and Pedersen, S. E. (1997) *Biochemistry 36*, 2068−2075.
16. Herz, J. M., Johnson, D. A., and Taylor, P. (1989) *J. Biol. Chem. 264*, 12439−12448.
17. Johnson, D. A., and Nuss, J. M. (1994) *Biochemistry 33*, 9070−9077.
18. Witzemann, V., and Raftery, M. (1978) *Biochemistry 17*, 3598−3604.
19. Pedersen, S. E., Dreyer, E. B., and Cohen, J. B. (1986) *J. Biol. Chem. 261*, 13735−13743.
20. Blanton, M. P., and Cohen, J. B. (1994) *Biochemistry 33*, 2859−2872.
21. Middleton, R. E., and Cohen, J. B. (1991) *Biochemistry 30*, 6987−6997.
22. Schagger, H., and von Jagow, G. (1987) *Anal. Biochem. 166*, 368−379.
23. Carr, C., Fischbach, G. D., and Cohen, J. B. (1989) *J. Cell. Biol. 109*, 1753−1764.
24. Blanton, M. P., Xie, Y., Dangott, L. J., and Cohen, J. B. (1999) *Mol. Pharmacol. 55*, 269−278.
25. Blanton, M. P., Li, Y. M., Stimson, E. R., Maggio, J. E., and Cohen, J. B. (1994) *Mol. Pharmacol. 46*, 1048−1055.
26. Strecker, A., Franke, P., Weise, C., and Hucho, F. (1994) *Eur. J. Biochem. 220*, 1005−1011.
27. Akabas, M. H., Kaufmann, C., Archdeacon, P., and Karlin, A. (1994) *Neuron 13*, 919−927.
28. White, B. H., and Cohen, J. B. (1992) *J. Biol. Chem. 267*, 15770−15783.
29. Giraudat, J., Dennis, M., Heidmann, T., Chang, J.-Y., and Changeux, J.-P. (1986) *Proc. Natl. Acad. Sci. U.S.A. 83*, 2719−2723.
30. Giraudat, J., Dennis, M., Heidmann, T., Haumont, P.-Y., Lederer, F., and Changeux, J.-P. (1987) *Biochemistry 26*, 2410−2418.
31. Bayley, H. (1983) *Photoregenerated reagents in biochemistry and molecular biology*, Elsevier, Amsterdam.
32. Unwin, N. (1993) *J. Mol. Biol. 229*, 1101−1124.

BI0011680